Insertion and Orientation of a Synthetic Peptide Representing the C-Terminus of the A_1 Domain of Shiga Toxin into Phospholipid Membranes†

Mazen T. Saleh,‡ Jim Ferguson,‡ Joan M. Boggs,§ and Jean Gariépy*,‡

Department of Medical Biophysics, University of Toronto and the Ontario Cancer Institute, 610 University Avenue, Toronto, Canada M5G 2M9, and Department of Biochemistry, University of Toronto and the Hospital for Sick Children, 555 University Avenue, Toronto, Canada M5G 1X8

Received January 24, 1996; Revised Manuscript Received May 6, 1996⊗

ABSTRACT: Shiga toxin is a bacterial protein composed of one A and five B subunits. Its A chain possesses a protease sensitive loop (Cys-242−Cys-261) that is cleaved to produce an enzymatically active A_1 domain and an A_2 fragment associated with its B subunit pentamer. The proposed mode of action of the toxin is linked to its retrograde transport to the ER lumen followed by the translocation of its catalytic A_1 chain to the cytoplasmic side of the ER membrane. A signal sequence-like domain (residues 220−246) which constitutes the C-terminus of the A_1 chain precedes a region within the protease sensitive loop (residues 247−258) that contains known and putative cleavage sites. Two peptides corresponding to this C-terminus (residues 220−246) were chemically synthesized to investigate if this signal sequence-like domain can interact with membranes. Such a property may provide a clue to the mechanism of translocation of the A_1 domain across the ER membrane. The first peptide represented the native sequence, which includes a naturally occurring cysteine at position 242 and provided a thiol moiety for the attachment of a spin-label. A second peptide was designed to contain a single tryptophan residue (Ile232Trp) located within the hydrophobic core of the sequence which served as an intrinsic fluorescence probe. The interactions of both peptides with lipid vesicles were analyzed by circular dichroism, fluorescence, and EPR spectroscopy. The peptides lack structure in aqueous buffers and adopted an α-helical geometry when bound to negatively charged lipid vesicles. The addition of lipid vesicles to a solution of the tryptophan-containing peptide results in a blue shift in the wavelength of its fluorescence maxima as well as an increase in fluorescence intensity at 335 nm, suggesting that the hydrophobic core of this A_1 peptide relocated to a nonpolar environment. EPR measurements of a proxyl-labeled analog of the peptide (introduced at Cys-242) indicated a decreased mobility of a fraction of the proxyl probe in the presence of lipid vesicles. At pH 7, the membrane-bound probe was completely reduced by ascorbate trapped inside vesicles but only partially reduced by ascorbate added outside the vesicles, suggesting that the C-terminal region of the peptide traversed the membrane bilayer or relocated close to the surface of its inner lipid leaflet. Finally, the peptide was shown to insert into lipid vesicles, causing the release of calcein at a high peptide:lipid ratio. These results suggest that the C-terminal tail of the A_1 chain may anchor this domain into the ER membrane.

Shiga toxin (ShT),[1] produced by *Shigella dysenteriae* type 1, and Shiga-like toxin (SLT), produced by pathogenic strains of *Escherichia coli*, are closely related bipartite protein toxins (O'Brien et al., 1987). These toxins share structural and functional properties with other plant and bacterial toxins such as diphtheria toxin, *Pseudomonas* exotoxin A, and ricin [for review, see Merritt and Hol (1995)]. All members of these toxin families possess an enzymatic domain and a receptor binding domain which are encoded by separate subunits.

ShT binds to cells expressing the glycolipid receptor, globotriosyl ceramide (Gb_3; Jacewicz et al., 1986; Lindberg et al., 1987). Following receptor binding, ShT is internalized via receptor-mediated endocytosis. A protease sensitive loop has been identified near the C-terminal region of the A subunit and is delimited by a disulfide bond between Cys-242 and Cys-261. During intracellular localization events, the 31 kDa A chain is reduced and cleaved to yield two fragments (Garred et al., 1995a), namely a 27 kDa A_1 domain which possesses a *N*-glycosidase activity and a 4 kDa C-terminal A_2 fragment partly inserted into the central pore of a B subunit pentamer (Fraser et al., 1994). A fraction of the processed toxin is rerouted by retrograde transport through the Golgi cisternae, the endoplasmic reticulum (ER), and the nuclear membrane (Sandvig et al., 1991, 1992). The blockage of retrograde transport with brefeldin A protects cells sensitive to the action of ShT and suggests that the toxin must reach the lumenal compartments of the Golgi network and the ER before its A_1 subunit can be effectively

† This work was supported by Grant MT-11218 from the Medical Research Council of Canada.

* Correspondence should be addressed to this author. Telephone: 416-946-2967. Fax: 416-946-6529. E-mail: gariepy@oci.utoronto.ca.

‡ University of Toronto and the Ontario Cancer Institute.

§ University of Toronto and the Hospital for Sick Children.

⊗ Abstract published in *Advance ACS Abstracts,* July 1, 1996.

[1] Abbreviations: DMPC, dimyristoylphosphatidylcholine; DMPG, dimyristoylphosphatidylglycerol; EPR, electron paramagnetic resonance; ShT, Shiga toxin; SLT, Shiga-like toxin; ShTA(220−246), 27-amino acid long synthetic peptide representing residues 220−246 of the ShT A chain; $W^{232}A^{242}$ShTA(220−246), peptide analog of ShTA(220−246) with an Ile → Trp substitution at position 232 and a Cys → Ala substitution at position 242; SUV, small unilamellar vesicles; TFE, trifluoroethanol.

S0006-2960(96)00177-8 CCC: $12.00

translocated near ribosomal subunits (Garred et al., 1995b). Since the target site for the *N*-glycosidase activity of the A_1 chain is a single adenine base of 28S rRNA (Endo et al., 1988; Saxena et al., 1989), the A_1 subunit must possess a mechanism to translocate to the cytoplasmic side of the ER membrane. In the case of diphtheria toxin, there is evidence that the toxin exploits the acidification of the endosomal compartment to undergo a conformational change and exposes a hydrophobic domain that enables it to translocate across membranes (Donovan et al., 1981; Hu et al., 1984; Blewitt et al., 1985; Rolf et al., 1993). A similar effect has been observed in the case of *Pseudomonas* exotoxin A where low pH alters its structure to reveal a membrane binding domain (Farahbakhsh & Wisnieski, 1989). Other toxins such as ShT and ricin appear to lack a response to endosomal pH and may have developed an alternate mechanism for relocating their enzymatic domain to the cytosol. One possible mechanism is the exposure of a hydrophobic domain during relocation of such toxins to the ER. ShT contains a segment (residues 247−258) within a protease sensitive loop (residues 242−261) which includes a well-defined furin sensitive motif RXXR (Gordon & Leppla, 1994) as well as putative cathepsins B and D cleavage sites. Proteolytic cleavage at multiple sites within this segment takes place during the intravesicular trafficking of the toxin (Takao et al., 1988; Blum et al., 1991; Burgess & Roberts, 1993; Garred et al., 1995a,b). An inspection of the A chain sequence of ShT and related toxins reveals the presence of a hydrophobic signal- sequence-like domain between residues 220 and 246 (this report; Figure 1). This region contains residues usually found in signal peptides and transmembrane protein segments (Perlman & Havorson, 1983; Briggs & Gierash, 1986) and constitutes the C-terminus of the A_1 fragment since it immediately precedes the start of the protease sensitive loop (Cys-242−Cys-261). The crystal structure of native Shiga toxin shows that this hydrophobic segment of the A subunit is hidden at the interface between the A subunit and the B subunit pentamer (Fraser et al., 1994). In the case of ricin, the isolated A subunit shows higher avidity for membranes than the holotoxin, indicating the exposure of a hydrophobic domain upon dissociation from the B subunit (Ishida et al., 1983; Utsumi et al., 1984, 1989; Yamasaki et al., 1988; Bilge et al., 1995). We therefore hypothesize that the reduction of the single disulfide bond of the A chain of ShT and its limited proteolysis may facilitate the release of the A_1 fragment from the holotoxin and/or expose its hydrophobic C-terminus, thus favoring its interaction with membranes.

In an effort to study the potential of the C-terminus tail of the A_1 domain to interact with membranes, we have synthesized peptides corresponding to residues 220−246 of the ShT A subunit and characterized their interaction with small unilamellar vesicles (SUV). We report spectroscopic results which demonstrate that this region of the A_1 domain inserts into negatively charged membranes and assumes an α-helical structure with a large fraction of the bound peptide spanning the width of a negatively charged lipid bilayer at neutral pH.

EXPERIMENTAL PROCEDURES

Materials. Dimyristoylphosphatidylglycerol (DMPG), dimyristoylphosphatidylcholine (DMPC), 3-maleimido-proxyl, and melittin were purchased from Sigma Chemical Co. (St. Louis, MO). Acetic anhydride (1-^{14}C) was obtained from Amersham Life Sciences (Arlington Heights, IL). Calcein was purchased from Molecular Probes Inc. (Eugene, OR). Morpholinoethanesulfonic acid (MES) was purchased from Fluka Chemical Corp. (St. Louis, MO).

Peptide Synthesis and Purification. The peptides were assembled by solid phase synthesis on an Applied Biosystems 431 peptide synthesizer using FMOC chemistry. The following peptides were synthesized: ShTA(220−246), [^{14}C]Ac-RVGRISFGSINAILGSVALILNCHHHA, which represents residues 220−246 in the native toxin and $W^{232}A^{242}$ShTA(220−246), [^{14}C]Ac-RVGRISFGSINAWLGS-VALILNAHHHA, which contains two substitutions, namely I232W and C242A. The N-terminus of each peptide was acetylated by reacting 100 mg of peptide-resin suspended in dichloromethane with 250 μCi of [1-^{14}C]acetic anhydride overnight at room temperature. The acetylation step was completed by further treating the sample with 10% (v/v) cold acetic anhydride in dichloromethane for 30 min prior to cleaving the peptides from the resin. The peptides were purified by reverse phase HPLC on a C_{18} column [Beckman ODS; 1 cm outside diameter × 25 cm; column was pre-equilibrated in water/0.1% (v/v) TFA] and eluted with a linear gradient of acetonitrile (AcN)/0.08% (v/v) TFA. The steepness of the elution gradient was 1% AcN/min. Both peptides typically eluted from the column when the composition of the mobile phase reached 60% acetonitrile. The column flow rate was 1 mL/min. The composition of each purified peptide was confirmed by amino acid analysis and mass spectrometry. The molar absorption coefficient of $W^{232}A^{242}$ShTA(220−246) at 280 nm was calculated to be 5700 M^{-1} cm^{-1}. The concentration of the melittin stock solution was calculated using the Trp molar absorption coefficient of 5570 M^{-1} cm^{-1} at 280 nm (Wetlaufer, 1962). The specific activity of the ^{14}C-labeled peptides was calculated to be 8.6×10^2 cpm/μg for $W^{232}A^{242}$ShTA(220−246) and 9.8×10^2 cpm/μg for ShTA(220−246).

Circular Dichroism. CD spectra were recorded at room temperature using an AVIV CD spectrometer model 62A DS. A 15 μL aliquot of a 2−4 mM stock solution of either peptide dissolved in 50% (v/v) TFE was diluted to a final volume of 2.8 mL in either 5 mM phosphate (pH 7.0) or 5 mM acetate (pH 5.0) and dispensed into a 1 cm path length cuvette. The final peptide concentration was typically between 10 and 20 μM. Spectra were collected with an averaging time period of 10 s per point. Each point represents the averaged ellipticity value recorded over a 0.5 nm spectral interval. When spectra were recorded in the presence of lipids, the peptide was added directly to a cuvette containing lipid vesicles suspended in a constantly stirring solution. Estimates of the helical fraction of the peptide were calculated by the method of Greenfield and Fasman (1969) using the following equation:

$$F_{\text{helix}} = \frac{[\theta]_{222}^{\text{obs}} - [\theta]_{222}^{\text{coil}}}{[\theta]_{222}^{\text{helix}} - [\theta]_{222}^{\text{coil}}}$$

where the value of $[\theta]_{222}^{\text{helix}}$ for a 27-amino acid long peptide was calculated to be −35 740 deg cm^2 $dmol^{-1}$ and the value for $[\theta]_{222}^{\text{coil}}$ was determined from a peptide solution prepared in 6 M guanidine hydrochloride.

Fluorescence Spectroscopy. Measurements were collected on a Photon Technology International (PTI) fluorometer.

Titration experiments were performed by adding 15 μL aliquots of preformed vesicles (5 mg/mL) suspended in either 5 mM phosphate (pH 7.0) or 5 mM acetate (pH 5.0) to a 1 cm path length cuvette containing the peptide $W^{232}A^{242}$ShTA-(220−246) (3 μM) dissolved in 2.8 mL of the same buffer. The resulting solution was continuously stirred while spectra were acquired. The excitation wavelength was set at 280 nm, and tryptophan emission spectra were recorded from 300 to 420 nm. In the case of experiments involving calcein leakage from lipid vesicles, the excitation wavelength used was 490 nm and the emission signal was monitored at 520 nm.

Proxyl Labeling of ShTA(220−246) Peptide. Purified peptide (1.0 mg) dissolved in 160 μL of 8 M urea and 40 μL of 3-maleimido-proxyl (10 mg/mL in methanol) were mixed together to give a 5-fold molar excess of the maleimido-proxyl group over the reactive thiol side chain (Cys-242) of ShTA(220−246). Fifty microliters of 0.25 M MES buffer (pH 6.2) was then added to the mixture and the reaction left to proceed overnight at room temperature. Excess proxyl label was removed by reverse phase HPLC using a semipreparative C_{18} column (Beckman ODS; 1 cm outside diameter × 25 cm). The column was developed with a linear gradient from 0 to 100% acetonitrile/0.08% TFA. The steepness of the gradient was 1% AcN/min, and the proxyl-labeled peptide eluted from the column when the composition of the mobile phase reached 60% acetonitrile. The column flow rate was 1 mL/min. The concentration of proxyl-ShTA(220−246) samples was determined by integrating the EPR spectra and comparing the spectral signals to that of a free maleimido-proxyl standard dissolved in 5 mM phosphate (pH 7.0). From this analysis, the molar ratio of proxyl group coupled to peptide was determined to be 0.83.

EPR Measurements. Spectra were collected using a Varian E-104B EPR spectrometer operated in continuous wave mode and equipped with a Varian variable-temperature module. Samples were contained in a sealed 50 μL glass micropipette. The peptide concentrations used were typically 20−30 μM, and the peptide:lipid molar ratio was maintained constant at 1:120. Ascorbic acid causes the reduction of the spin-label free radical, thus abolishing its EPR spectrum. In the case of ascorbate reduction experiments, 2 μL of 1.0 M sodium ascorbate prepared in either 5 mM phosphate (pH 7.0) or 5 mM acetate (pH 5.0) buffers was added to 120 μL of the peptide/vesicle mixture immediately before data collection. In some reduction experiments, ascorbate ions were entrapped into SUV during vesicle formation and the loaded vesicles purified from free ascorbate ions by gel filtration chromatography as described below for calcein. Peptide solutions were then mixed with loaded SUV just prior to data acquisition. For fast, nearly isotropic motion, the motional parameter τ_o was obtained as described elsewhere (Eletr & Keith, 1972). In the case of spectra reflecting slower motion, relative changes in motion were determined from the maximum hyperfine splitting, T_{max}. However, due to the low amplitude of the spectra and broadness of the outer high-field peak, this value was measured as the separation of the outer low-field line from the midpoint of the center peak where it crossed the baseline, rather than as $^1/_2$ the separation of the outer low-field line from the outer high-field line.

Preparation of Small Unilamellar Vesicles. DMPG or DMPC was dispensed from a lipid stock solution (500 μL of a 20 mg/mL solution) prepared in chloroform/methanol (1:1) into a 16 × 125 mm borosilicate test tube and dried under a stream of nitrogen. Residual solvents were removed under vacuum for 3 h. The lipid films were then resuspended and hydrated in 2 mL of either 5 mM phosphate (pH 7.0) or 5 mM acetate (pH 5.0) using 10 cycles of fast freeze−thaw (Mayer et al., 1985). The large multilamellar vesicles formed were then subjected to sonication in a bath sonicator to visual clarity. The small unilamellar vesicles (SUV) produced by this procedure were used directly in the experiments. For calcein leakage experiments, the vesicles were formed in the presence of 20 mM calcein, after which the free calcein was removed by gel filtration on a Sephadex G15 column (1.5 cm × 40 cm) and eluted using the same buffer in which the vesicles were prepared.

Binding of Radiolabeled Peptide to Lipid Vesicles. $W^{232}A^{242}$ShTA(220−246) samples [42 μg dissolved in either 5 mM phosphate (pH 7.0) or 5 mM acetate (pH 5.0); specific activity, 8.6×10^2 cpm/μg] were dispensed into centrifuge tubes (13 × 51 mm; Beckman, polyallomer). Increasing amounts of preformed DMPG or DMPC vesicles suspended in the same buffer were then added to the tubes to reach a final volume of 4.0 mL. The tubes were then centrifuged at 175000*g* for 5 h, and the radioactivity of the supernatant was measured (Wang et al., 1993). Lipid concentrations were determined by the phosphorus assay (Rouser et al., 1975). The fraction of peptide bound to vesicles was calculated as $1 - S_{lipid}/S_{total}$, where S_{lipid} represents the radioactivity (in counts per minute) associated with the supernatant recovered from centrifuging samples containing the ^{14}C-labeled peptide in the presence of lipid vesicles at a peptide:lipid molar ratio of 1:50. The term S_{total} represents the radioactivity (in counts per minute) recorded for control supernatants (radiolabeled peptide in the absence of lipid vesicles).

RESULTS AND DISCUSSION

The A_1 chain of Shiga and related toxins must transit from the lumenal side of the endoplasmic reticulum to the cytoplasmic side to be able to effectively interact with ribosomal subunits and block protein synthesis. This translocation event may be initiated by a specific domain of the toxin as in the case of other bacterial toxins (*Pseudomonas* exotoxin A, diphtheria toxin). Such a domain has not been identified in bacterial toxins such as Shiga and Shiga-like toxins. We propose that the C-terminus created as a result of proteolysis and reduction of the A chain in this toxin family may represent a functional domain triggering membrane translocation. Recently, a proline mutation (Pro250Ala) in a 12-residue hydrophobic segment located near the C-terminus of the A chain of ricin has been shown to affect the ability of ricin to intoxicate Vero cells but did not affect its *N*-glycosidase activity (Simpson et al., 1995). This finding was interpreted as suggesting that this hydrophobic domain may be involved in membrane translocation. A representation of the A chain of Shiga toxin in Figure 1 (panels A and B) highlights the presence of a proteolytic loop (Cys-242−Cys-261) flanked on its amino terminus by a 27-amino acid long signal sequence-like domain (residues 220−246). This domain represents the C-terminus of the A_1 subunit created as the result of transcytosis modifications.

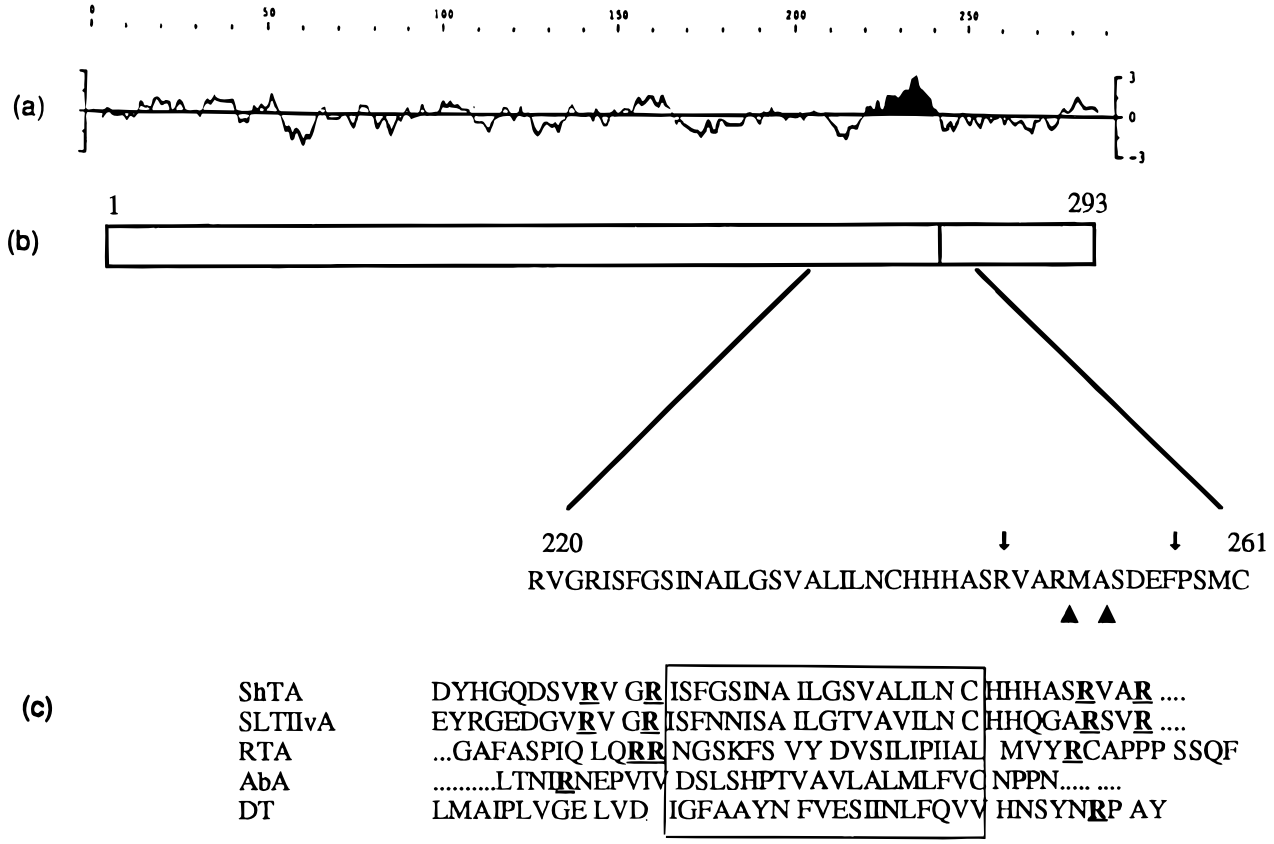

FIGURE 1: (a) Hydrophobicity profile of the A subunit of Shiga toxin (ShT) using the Goldman, Engelman, and Steitz (GES) scale (Engelman et al., 1986). The A chain of Shiga toxin is proteolytically cleaved into two domains, namely a catalytic A_1 domain and a short A_2 domain associated with the binding subunit of the toxin. The shaded area in the hydrophobicity profile identifies the sequence from residues 225 to 242 as representing the most dominant hydrophobic region of the A_1 chain. (b) Schematic representation of ShT subunit organization showing the relative location of the hydrophobic region in relation to the known protease sensitive loop (Cys-242−Cys-261). Established (▲) and putative (cathepsins B and D; ↓) cleavage sites within the loop are highlighted on the amino acid sequence. (c) Sequence alignment of the C-terminus of ShT A_1 with regions of other ribosome-inhibiting toxins. Abbreviations and sequences listed in this panel are associated with the following toxins: SLTIIv, residues 212−251 of the A subunit of the Shiga-like toxin II variant; RTA, residues 225−268 of the A chain of ricin; AbA, residues 217−249 of the A subunit of abrin; and DT, residues 341−380 of diphtheria toxin. Several protein toxins possess a stretch of hydrophobic amino acids (boxed sequences) flanked by positively charged amino acids (bold, underlined) at neutral pH.

The hydrophobicity profile of the A chain [Figure 1A; derived using the method of Engelman et al. (1986)] further suggests that this domain (darkened area) may represent a transmembrane region. Sequence alignments of Shiga and related toxins (Figure 1C) with a segment of the A chain of ricin implicated in membrane translocation (Simpson et al., 1995) illustrate the existence of a common hydrophobic region within these molecules. Ricin and Shiga toxins have A chains with homologous functions. The crystal structure of Shiga toxin shows that there are a limited number of interactions between its A_1 domain and the B subunit pentamer. In particular, residues 226−242 are buried under most of the A_1 subunit, in close proximity to the B pentamer, but making no contact with the pentamer (Fraser et al., 1994). Thus, most of the C-terminus of the A_1 chain is not initially accessible to solvent as part of the intact toxin. We hypothesize that this domain becomes exposed after cleaving the protease sensitive loop at one or more sites and reducing the disulfide bridge between Cys-242 and Cys-261. The newly created signal sequence-like C-terminus may then possess membrane active properties that would facilitate the A_1 chain insertion from the lumenal side of the Golgi or ER membranes.

In this study, peptides were synthesized to investigate the ability of this region of the A_1 domain to interact and insert into phospholipid membranes. Two peptides representing residues 220−246 of the A_1 domain were assembled by solid phase peptide synthesis. Their amino terminus was acetylated with acetic anhydride to ensure the absence of an unnatural positive charge. The peptide ShTA(220−246) includes a naturally occurring cysteine residue at position 242 which provided a unique site for the subsequent incorporation of a paramagnetic probe (proxyl group) to monitor the insertion and orientation of the peptide into unilamellar vesicles. The peptide analog, $W^{232}A^{242}$ShTA-(220−246), included two mutations, namely Cys242Ala and Ile232Trp, to monitor its interaction with membranes by fluorescence spectroscopy. Spectroscopic experiments were performed at two pH values, namely 5.0 and 7.0, to mimic representative pH conditions observed in endosomal and ER compartments, respectively.

ShTA(220−246) Adopts a Partially Helical Structure in the Presence of Negatively Charged Lipid Vesicles. The circular dichroism spectrum of ShTA(220−246) dissolved in 5 mM phosphate (pH 7.0) suggests that this peptide lacks structure (random coil) in aqueous solutions (Figure 2). The mean residue ellipticity (MRE) at 222 nm was experimentally determined to be -5000 ± 600 deg cm^2 dmol^{-1}. The propensity of ShTA(220−246) to adopt a partially α-helical conformation in hydrophobic environments was demonstrated

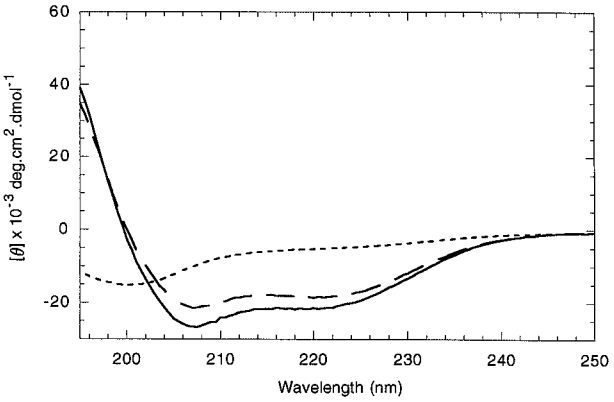

FIGURE 2: Circular dichroism spectra of the peptide ShTA(220−246) dissolved either in 5 mM phosphate (pH 7.0) (- - -), in 10% (w/v) SDS (− −), or in 50% (v/v) TFE (—). The peptide concentration was 15 μM.

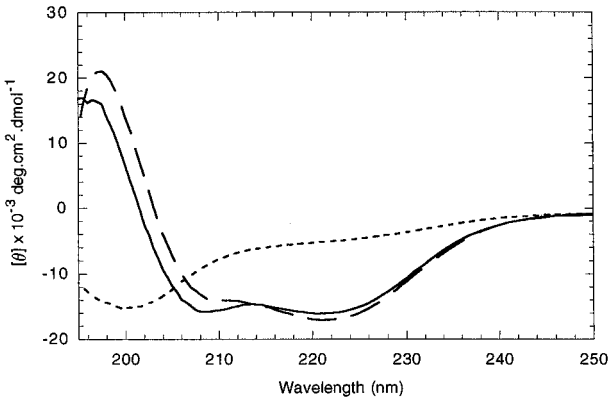

FIGURE 3: Circular dichroism spectra of the peptide ShTA(220−246) in the presence of small unilamellar vesicles composed of DMPG lipids. The spectrum of the peptide dissolved in 5 mM phosphate buffer (pH 7.0) (- - -) is compared to that of the peptide exposed to DMPG vesicles at pH 7.0 (—) and pH 5.0 (− −). The peptide concentration was 15 μM.

in the presence of SDS micelles (MRE of $-18\,000 \pm 900$ deg cm^2 dmol^{-1} at 222 nm). This finding was further supported by recording the spectrum of the peptide in 50% (v/v) TFE, where the ellipticity maximum at 222 nm reached a value of $-22\,000 \pm 1100$ deg cm^2 dmol^{-1}. The peptide also assumed a partially α-helical structure in the presence of vesicles constructed with negatively charged lipids (DMPG; Figure 3). Similar CD spectra were recorded at pH 5.0 and 7.0, with a negative maximum at 222 nm of $16\,750 \pm 1200$ deg cm^2 dmol^{-1} at a peptide:lipid ratio of 1:50. This ellipticity value translates to an approximate helical content of 45−50%. This finding indicates that the membrane-bound peptide is mostly α-helical in structure at pH 7.0 and to a lesser extent at pH 5.0. In the presence of vesicles composed of neutral lipids such as DMPC, the peptide appears to possess significantly less α-helical character with a MRE$^{222\ nm}$ of $-11\,000 \pm 850$ deg cm^2 dmol^{-1} at pH 7.0 and half that value at pH 5.0 (Figure 4). A broad negative maximum centered at 218 nm was observed in the spectrum of ShTA(220−246) exposed to DMPC vesicles at pH 7.0 and suggests the existence of one or more peptide conformations that would include β-sheet-containing structures. ShTA(220−246) tends to slowly aggregate in aqueous buffers (hours), giving rise to a circular dichroism spectrum showing a minimum between 213 and 218 nm, a characteristic feature of β-sheet structure (data not shown). Aggregation may be nucleated by the presence of DMPC

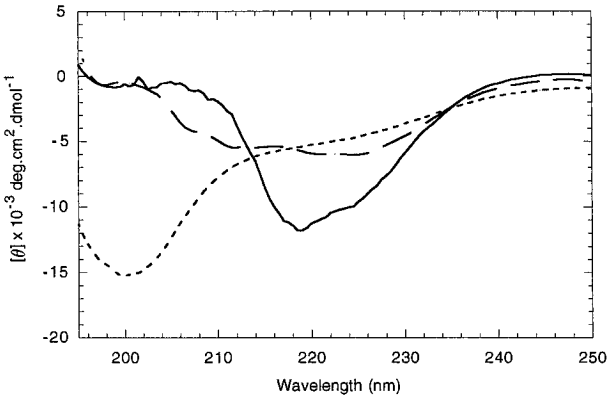

FIGURE 4: Circular dichroism spectra of the peptide ShTA(220−246) in the presence of small unilamellar vesicles composed of DMPC lipids. The spectrum of the peptide dissolved in 5 mM phosphate buffer (pH 7.0) (- - -) is compared to that of the peptide exposed to DMPC vesicles at pH 7.0 (—) and pH 5.0 (− −). The peptide concentration was 15 μM.

vesicles at pH 7.0. Similar circular dichroism results were recorded for the peptide analog W^{232}A^{242}ShTA(220−246) (data not shown).

Changes in the Fluorescence Spectrum of W^{232}A^{242}ShTA-(220−246) in the Presence of Lipid Vesicles Suggest That This Hydrophobic Region of the A_1 Domain Partitions Readily into a Lipid Bilayer. Substituting isoleucine with tryptophan at position 232 provided us with an intrinsic probe to monitor the environment of the hydrophobic core of the peptide. The Trp emission spectra of the peptide in solution showed a maximum at 354 nm, indicating that the tryptophan side chain was exposed to the aqueous environment. As DMPG vesicles were added to the peptide solution at pH 7.0, a blue shift (354 to 335 nm) in the emission maxima of the peptide was observed (Figure 5A), indicating that the Trp side chain had migrated to a hydrophobic environment (Lakowicz, 1983). Changes in the fluorescence intensity at 335 nm (F/F_o) were also monitored as a function of lipid concentration (Figure 5B). The increase in fluorescence intensity correlated with the observed spectral shift to 335 nm (Figure 5A). Both measurements support the concept that the indole ring has relocated to a hydrophobic environment (Wharton et al., 1988). Similar spectral characteristics were observed at pH 5.0 in the presence of DMPG vesicles. Changes in the spectra of W^{232}A^{242}ShTA(220−246) in the presence of DMPC vesicles at pH 7.0 were comparable to those observed in the presence of DMPG vesicles. However, these changes occurred at higher lipid:peptide ratios. These results were not observed for the peptide mixed with DMPC vesicles at pH 5.0. Mixtures of acidic and zwitterionic lipids were also used to mimic physiological conditions expected on the inner leaflet of the ER membrane. The composition of the inner leaflet of rat liver rough endoplasmic reticulum is dominated by zwitterionic (neutral) lipids such as phosphatidylcholine and phosphatidylethanolamine (Bollen & Higgins, 1980; Zachowski, 1993). However, acidic lipids such as phosphatidylserine, phosphatidylinositol, and phosphatidylglycerol account for 7−25% of the rough ER inner leaflet composition (Bollen & Higgins, 1980). This lipid leaflet is thus negatively charged. The association of W^{232}A^{242}ShTA(220−246) with such membranes was assessed using DMPC vesicles containing a level of DMPG (20:80 ratio, DMPG/DMPC) representative of the proportion of negatively charged lipid present in the rat liver ER inner

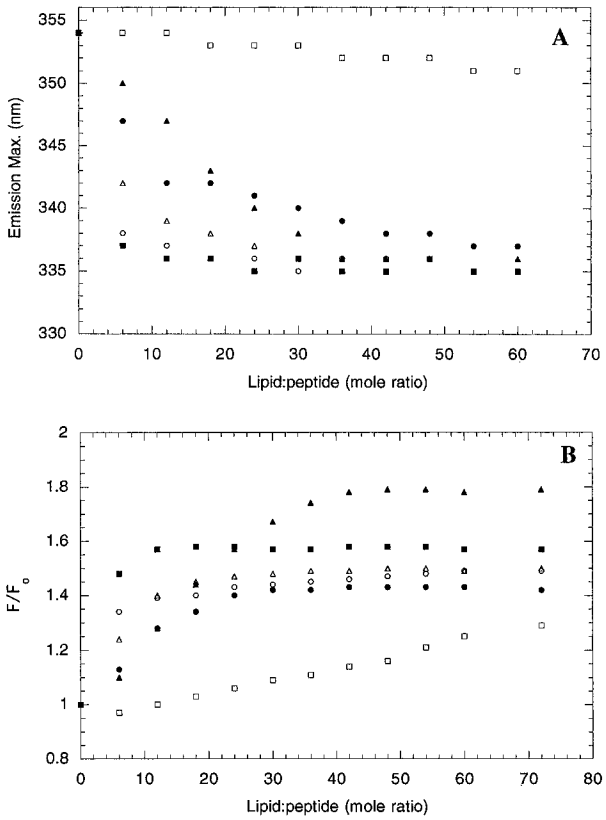

FIGURE 5: Effect of lipid concentration and composition on the tryptophan fluorescence emission spectra of $W^{232}A^{242}$ShTA(220−246). The fluorescence spectra of $W^{232}A^{242}$ShTA(220−246) were recorded in the presence of increasing amounts of vesicles containing either DMPG, DMPC, or a 20:80 DMPG/DMPC mixture at pH 7.0 and 5.0. The peptide concentration was 3 μM. (A) Effect of the lipid:peptide ratio on the tryptophan fluorescence emission maxima of $W^{232}A^{242}$ShTA(220−246): ○, DMPG (pH 7.0); ■, DMPG (pH. 5.0); ●, DMPC (pH 7.0); □, DMPC (pH 5.0); ▲, 20:80 DMPG/DMPC (pH 7.0); and △, 20:80 DMPG/DMPC (pH 5.0). (B) Effect of the lipid:peptide ratio on the tryptophan fluorescence intensity of $W^{232}A^{242}$ShTA(220−246). The excitation wavelength was set at 280 nm, and the F/F_o ratio was determined from the emission signal recorded at 335 nm: ○, DMPG (pH 7.0); ■, DMPG (pH. 5.0); ●, DMPC (pH 7.0); □, DMPC (pH 5.0); ▲, 20:80 DMPG/DMPC (pH 7.0); and △, 20:80 DMPG/DMPC (pH 5.0).

lipid leaflet. The effects on both the fluorescence intensity and shift in wavelength emission maximum of $W^{232}A^{242}$-ShTA(220−246) were similar to those observed for the peptide interacting with vesicles composed of DMPG lipids only (Figure 5A,B). When vesicles were constructed with a 5:95 ratio of DMPG to DMPC, the changes observed were intermediate to those recorded when $W^{232}A^{242}$ShTA(220−246) was added to either pure DMPG or DMPC vesicles alone (data not shown). The influence of mixed lipid vesicles on the fluorescence spectral properties of the peptide suggests that the presence of low levels of negatively charged lipids (such as DMPG) in membranes can strongly dictate the association of $W^{232}A^{242}$ShTA(220−246) with lipid vesicles.

Binding of Radiolabeled $W^{232}A^{242}$ShTA(220−246) to Lipid Vesicles. A [^{14}C]acetyl group was initially introduced at the N-terminus of $W^{232}A^{242}$ShTA(220−246) during synthesis. The radiolabeled peptide was shown by centrifugation to interact directly with small unilamellar vesicles. The fraction of bound peptide was determined to be 0.48 ± 0.09 at pH 7.0 and 0.51 ± 0.07 at pH 5.0 in the presence of DMPG vesicles, while values of 0.31 ± 0.07 at pH 7.0 and 0.1 ± 0.05 at pH 5.0, respectively, were calculated for the fraction

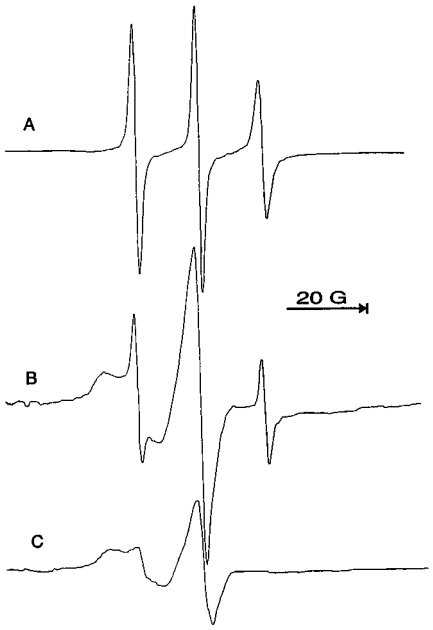

FIGURE 6: Effect of DMPG vesicles and ascorbic acid on the EPR spectrum of proxyl-labeled ShTA(220−246). The EPR spectrum of the labeled peptide was recorded for the peptide dissolved in 5 mM phosphate buffer (pH 7.0) (spectrum A), in the presence of DMPG vesicles suspended in the same buffer (spectrum B), and after the external addition of 12 mM (final concentration) ascorbic acid to the peptide/vesicles mixture (spectrum C).

of peptide bound to DMPC vesicles. These results suggest that $W^{232}A^{242}$ShTA(220−246) partitions more favorably into a membrane containing negatively charged lipids such as DMPG than in neutral lipids exemplified by DMPC. In addition, the reduced fraction of peptide bound to vesicles containing a zwitterionic lipid (DMPC) at pH 5.0 suggests that the protonation of the three C-terminal histidines of $W^{232}A^{242}$ShTA(220−246) may accentuate its partitioning into the aqueous phase.

Since the helical content of the peptide in the presence of DMPG vesicles at both pH 5.0 and 7.0 was estimated to be approximately 50% and that the CD spectrum of the peptide free in solution (Figures 2−4) lacks helical character, one can conclude that the population of membrane-bound peptide must adopt a mostly α-helical structure.

Monitoring the Interaction of ShTA(220−246) with Membranes by EPR. The naturally occurring cysteine residue located near the C-terminus of ShTA(220−246) provided a useful site to insert a paramagnetic proxyl group in the peptide. As monitored by EPR spectroscopy, the covalently attached proxyl probe displayed its expected isotropic mobility when the peptide was dissolved in an aqueous environment. The spectrum of the proxyl−peptide conjugate highlights the anticipated triplet of narrow spectral lines (Figure 6A). The value of the proxyl's motional parameter τ_o was significantly increased (Table 1, 0.30 ns) when compared to that of the free spin-label (0.02 ns), reflecting the fact that the probe is less mobile when bound to the peptide. When the labeled peptide was mixed with vesicles composed of the neutral lipid, DMPC, there was little effect on the spectrum of the probe except for a small increase in τ_o values (Table 1), suggesting that there was little interaction of the peptide with DMPC vesicles at pH 7.0. One or more monomers of DMPC may bind to the peptide in solution and decrease its motion. The circular dichroism spectrum of ShTA(220−246) observed in the presence of DMPC

Table 1: EPR Parameters Derived from Spectra of Spin-Labeled ShTA(220−246) in Different Environments[a]

sample	pH	temperature (°C)	T_{max} (G)	τ_o (ns)
free spin-label	7.0	26.5		0.02
spin-labeled peptide in buffer	7.0	6.5		0.45
		26.5		0.30
		37.5		0.23
spin-labeled peptide + DMPC vesicles	7.0	6.5		0.57
		26.5		0.36
		37.5		0.29
spin-labeled peptide + DMPG vesicles	7.0	6.5	26.3	
		26.5	23.4	
		37.5	20.1	
	5.0	6.5	25.9	
		26.5	24.4	
		37.5	23.4	

[a] Experimental conditions and the derivation of T_{max} and τ_o values are described in Experimental Procedures.

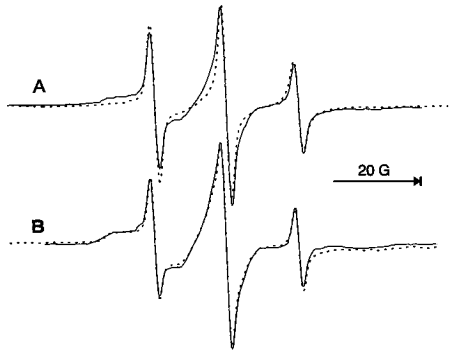

FIGURE 7: Reduction of only the immobilized EPR spectral component by entrapped ascorbic acid. Superimposed EPR spectra of the proxyl-labeled peptide in the presence of DMPG vesicles at pH 7.0 (part A, solid line spectrum) and of the labeled peptide interacting with DMPG vesicles loaded with ascorbic acid, at pH 7.0 (part A, dotted line spectrum). Superimposed EPR spectra of the proxyl-labeled peptide in the presence of DMPG vesicles at pH 5.0 (part B, solid line spectrum) and of the labeled peptide interacting with DMPG vesicles loaded with ascorbic acid, at pH 5.0 (part B, dotted line spectrum).

vesicles at pH 7.0 (Figure 4) suggests the existence of peptide conformers containing β-sheet structure and indirectly supports the presence of microaggregates of the peptide on the surface of DMPC vesicles. Such an event would explain our binding results where 31% of the peptide population was found to be associated with DMPC vesicles at a peptide: lipid ratio of 1:50. In the presence of negatively charged DMPG vesicles, the spectrum at 26.5 °C contained two spectral components (Figure 6B). One component (mobile component), representing the free peptide, was defined by the set of sharp lines previously observed in the spectrum of the proxyl−peptide in solution (Figure 6A). The other spectral component (immobilized component) was broader with greater hyperfine splitting and reflected the more restricted motion of the spin-labeled peptide bound to DMPG vesicles. The amount of immobilized component was greater at pH 5 than at pH 7 (parts A and B of Figure 7). The mobility of the spin-labeled peptide bound to DMPG rose with increasing temperatures, as indicated by a decrease in the value of the maximum hyperfine splitting parameter, T_{max} (Table 1). The lipid exists in the gel phase at 6.5 °C and in the liquid crystalline phase at 37.5 °C. There were no significant changes in line shape when the temperature of the peptide in solution was varied, indicating that the observed changes in the spectra with temperature in the presence of DMPG vesicles were not due to changes in the conformation of the free peptide, but rather due to its binding to the lipid bilayer. The change in mobility as a function of temperature was greater at pH 7 than at pH 5, suggesting that the spin-label on the peptide was more sensitive to the DMPG gel to liquid crystalline phase transition at pH 7 than at pH 5 (Table 1).

The preceding results demonstrate that the C-terminus of the peptide associates with DMPG membranes. This conclusion is supported by the motional restriction of the proxyl group and its sensitivity to the lipid phase transition. However, motional restriction could occur as a result of either peptide binding to the bilayer surface or peptide insertion into the bilayer. Addition of ascorbic acid (10−20 mM) to the outside of DMPG vesicles almost completely reduced the mobile spectral component (sharp lines) as shown in Figure 6C. Interestingly, only a partial reduction (at most 50%) of the immobilized component was observed at pH 7.0 (Figure 6C), indicating that only a fraction of the bound peptide C-terminus is accessible to ascorbic acid from the outside of vesicles. At pH 5, ∼70% of the immobilized component was reduced by externally added ascorbic acid (data not shown), suggesting a greater access of ascorbic acid to the probe. Ascorbic acid completely reduced the spectrum of the labeled peptide in the presence of DMPC vesicles, indicating that the spin-label is completely accessible to the aqueous phase in the presence of this neutral lipid.

Use of this peptide with a spin-label conjugated to cysteine at position 242 enabled us to determine the directionality of membrane insertion. To monitor if the C-terminus of the peptide could penetrate the bilayer of DMPG vesicles, the spin-labeled peptide was added to ascorbic acid-loaded vesicles at pH 7.0. In contrast to the effect of ascorbic acid added to the outside of the vesicles, the ascorbic acid (12 mM) trapped inside the vesicles caused an almost complete reduction of only the immobilized component of the spectrum, leaving the mobile component unaffected (Figure 7A). The addition of the spin-labeled peptide to vesicles containing ascorbic acid at pH 5.0 did not alter any components of the spin-label spectrum (Figure 7B). These results suggest that at pH 7 the C-terminus of the bound peptide is accessible to intravesicular ascorbic acid and may thus insert through the lipid bilayer. At pH 5, the proxyl group must reside mostly near the surface of the SUV outer leaflet (Figure 7B and preceding paragraph) where it is more accessible to ascorbate added outside the vesicles. The partial or complete protonation of the three C-terminal histidines (positions 243−245) at pH 5.0 may contribute to the lack of penetration of the peptide into the lipid bilayer, thus favoring the orientation of ShTA(220−246) along the surface of the membrane at endosomal/lysosomal pHs (pH 4.5−6.0).

ShTA(220−246) Causes Leakage of Calcein Trapped inside DMPG Vesicles. The C-terminus of the A_1 domain may possess membrane active properties. The addition of ShTA(220−246) to DMPG SUV at pH 7.0 containing self-quenching concentrations of calcein resulted in a rapid increase in fluorescence intensity at 520 nm, indicating the release of the calcein fluorophore. Similar results were recorded at pH 5.0 (data not shown). The release of calcein

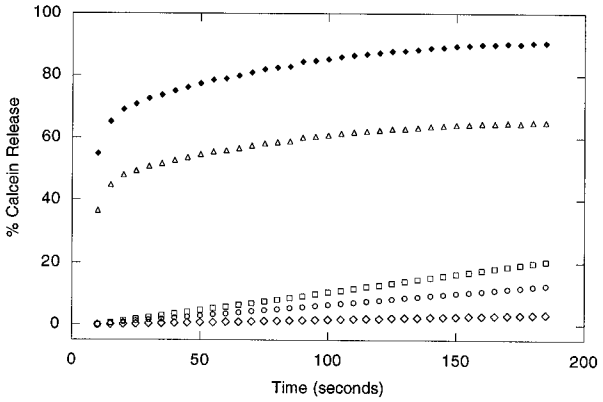

FIGURE 8: Peptide-induced leakage of calcein from DMPG vesicles as a function of time and peptide:lipid ratio. The peptide ShTA-(220−246) was added to a cuvette containing 5 mM phosphate buffer (pH 7.0) and calcein-loaded DMPG vesicles. The fluorescence excitation wavelength was set at 490 nm, and the increase in the emission signal due to the release of calcein was monitored at 520 nm. The molar ratio of ShTA(220−246):DMPG lipid was either 1:4 (◆), 1:17 (□), or 1:50 (○). As a positive control, the peptide melittin was used at a melittin:lipid molar ratio of 1:17 (△). A curve (◇) representing the background leakage of calcein from DMPG vesicles observed in the absence of peptide is also shown. The fluorescence signal corresponding to 100% release of calcein from DMPG vesicles was determined by adding Triton-X100 [1% (v/v) final concentration] to each peptide/lipid mixture.

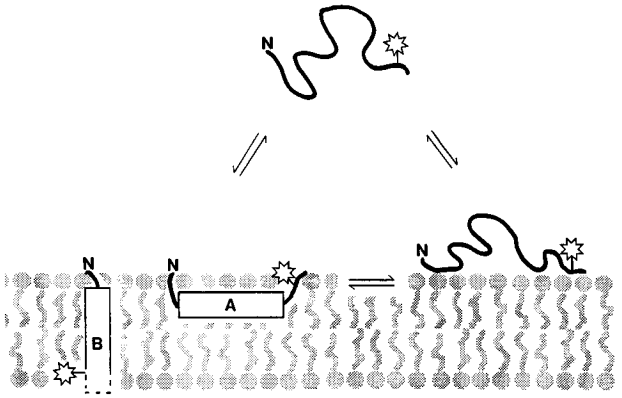

FIGURE 9: Schematic model depicting possible modes of interaction of peptide ShTA(220−246) with the lipid bilayer of DMPG vesicles. At pH 5, the dominant interaction is depicted by conformer A, where the peptide adopts a partially α-helical conformation and partitions within the bilayer with the helix axis being parallel to the normal axis of the membrane. At pH 7, a population of the peptide inserts and traverses the lipid bilayer (conformer B). Populations of both conformers A and B may exist at pH 7. The open star represents the position of the proxyl probe within the peptide, while the letter N indicates the location of its amino terminus. Open rectangles depict the length of the putative α-helical region within the peptide. The dotted line as part of the rectangle in conformer B represents an extension of the helical region beyond residue 242 (the site of incorporation of the proxyl label).

was observed at peptide:lipid molar ratios of 1:2 and 1:4 (1:4 ratio is shown in Figure 8). No significant leakage was observed at lower peptide:lipid ratios (1:17 or 1:50; Figure 8). Melittin, a pore-forming peptide used as a positive control, required peptide:lipid ratios on the order of 1:20 to achieve effects on vesicles loaded with calcein similar to those observed for ShTA(220−246) (Figure 8).

When DMPG vesicles were added to clear solutions of ShTA(220−246), the resulting mixtures became turbid at high peptide:lipid ratios, suggesting that the vesicles were starting to aggregate and fuse under such conditions. If the lipid vesicles were added to the peptide solution such that the peptide:lipid ratio was low (1:50), no turbidity was observed. Consistent with our calcein leakage experiments, this result indicates that leakage of calcein seen at a high peptide:lipid ratio may be the result of membrane insertion and disruption (detergent-like property) rather than channel formation.

Model Summarizing the Interaction of ShTA(220−246) with a Negatively Charged Lipid Bilayer. The results in this study indicate that the peptide representing the C-terminus of the A_1 fragment of ShT inserts into DMPG vesicles. Three possible types of interaction of ShTA(220−246) with a DMPG lipid bilayer are presented in Figure 9, which explain the restricted motion of the bound peptide and its sensitivity to the lipid phase transition. At pH 7, the N-terminus of ShT(220−246) is positively charged (Arg-220 and Arg-224) while its C-terminus remains mostly electrically neutral. Interactions of the peptide N-terminus with lipid head groups present on the outer leaflet of the vesicles are thus favored. The remaining segment of the peptide (residues 225−246) either may insert into the bilayer in an orientation parallel to the surface of the membrane (Figure 9, conformer A) or may traverse the lipid bilayer (Figure 9, conformer B). Results from fluorescence and circular dichroism spectroscopies cannot distinguish between conformers A and B since both membrane conformations would lead to the burying of the tryptophan side chain (fluorescence spectroscopy) and to the observation of a peptide adopting a mostly α-helical structure (circular dichroism). Only the EPR results presented in this study allow us to differentiate between such conformers. Most of the peptide population must traverse the DMPG bilayer with the C-terminus facing the interior of the vesicles since the C-terminus proxyl group (A) can be readily reduced by ascorbate entrapped inside vesicles and (B) is reduced to a much greater extent under such conditions than as a result of ascorbate being present on the outside of the vesicles. The putative transmembrane segment could include residues 225−246 (starting after Arg-224), suggesting that the resulting helix could incorporate up to 22 amino acids, a length sufficient to span most lipid bilayers (Persson & Argos, 1994; Rost et al., 1995). This hypothesis would imply that up to 81% (22 of 27 amino acids) of the peptide residues would have to adopt an α-helical conformation for the proxyl probe (Cys-242) to be located near the surface of the inner leaflet of a bilayer. Circular dichroism results and binding measurements of peptide to lipid vesicles predict that most of the residues in ShTA(220−246) bound to DMPG vesicles assume an α-helical geometry. More precisely, approximately half of the peptide is free in solution in equilibrium with the remaining peptide population existing as one or more α-helical membrane-bound conformers (as demonstrated by binding experiments, circular dichroism, and EPR results; Figures 3 and 6). In summary, the dominant ShTA(220−246) conformer bound to DMPG vesicles at pH 7.0 would be conformer B (Figure 9).

At pH 5.0, both the N- and C-termini are positively charged (Arg-220 and -224; His-243, -244, and -245). Reduction experiments with ascorbic acid indicate that the C-terminus of ShTA(220−246) is only accessible from the outer surface of the lipid vesicles, suggesting that the peptide does not traverse the bilayer at pH 5.0. The association of ShTA(220−246) with lipid vesicles at pH 5.0 was confirmed by circular dichroism, fluorescence, and binding experiments

with radiolabeled peptide. Thus, the hydrophobic core of the peptide probably inserts into the lipid bilayer in an orientation best depicted by conformer A (parallel to the surface of the bilayer) with its charged termini bound to negatively charged lipid head groups (Figure 9). Since the toxin must travel through acidic compartments (pH 5−6) prior to reaching the ER lumen (neutral pH), the insertion of the A_1 C-terminus into negatively charged membranes may be restricted to a particular orientation during the transit stage.

Finally, oriented CD measurements of magainins, a family of 23-residue frog peptides with antimicrobial properties, demonstrated that they adopt an α-helical conformation with two distinct orientations in relation to a lipid membrane (inserted either parallel or perpendicular to the lipid bilayer) (Ludtke et al., 1994). This report supports our results that membrane-bound ShTA(220−246) can insert into a lipid bilayer in the two proposed orientations.

Domains Analogous to ShTA(220−246) Are Present on Other Proteins. Amino acid sequences similar to our peptide sequence can be found in a number of proteins. In particular, the fusion of a related peptide present in the sequence of the human asialoglycoprotein (ASGP) receptor H1 (residues 38−65) to the C-terminal domain of rat α-tubulin resulted in the membrane insertion and translocation of the resulting protein construct (Spiess & Lodish, 1986). The presence of such a hydrophobic segment is also seen in the C-terminus of polyomavirus middle-T antigen (residues 394−421) which is involved in membrane binding (Markland et al., 1986). In the case of diphtheria toxin, the hydrophobic sequence shown in Figure 1 is located within the putative membrane translocation domain (Moskaug et al., 1991; Choe et al., 1992). Point mutation studies on this domain have revealed that substituting glutamic acid at position 362 with lysine allowed the toxin to translocate at a higher pH than the wild type (Falnes et al., 1992). More recently, spin-labeled analogs of the isolated transmembrane domain of diphtheria toxin have been shown to insert into and permeabilize large unilamellar vesicles (Zhan et al., 1995).

Do ShTA(220−246) and the A_1 Chain Interact with Component(s) of a Protein Transporter Located in the ER Membrane? The import of nascent protein chains associated with ribosomes into the ER lumen is thought to involve the recognition of signal sequences on newly synthesized proteins by a signal sequence binding protein (itself an ER membrane protein) in association with other known components of the protein translocation machinery to the ER [signal recognition particle (SRP), SRP receptor, ribosome, and transmembrane channel protein]. One hypothetical scenario may be that the C-terminus of the ShT A_1 domain inserts into the ER membrane and allows the catalytic domain to diffuse along the plane of the membrane until it is recognized by a signal sequence binding protein. Subunits of the transmembrane channel protein or recently assembled channel proteins may then be recruited or be already positioned in proximity to the complex of the ShT A_1 domain and the signal sequence binding protein, favoring the ultimate translocation of the A_1 domain across the ER membrane. As a result of interactions with the ER membrane and associated protein components, the population of bound A_1 chain may exist as a series of partly unfolded intermediates, which may then be recognized as appropriate substrates for export (cytosol) through the transmembrane protein channel. Finally, the involvement of various ER protein factors linked to the folding of proteins such as the protein disulfide isomerase, p88 or calnexin, HSP47, GRP94, and BiP (Gething & Sambrook, 1992; Gaut & Hendershot, 1993; Simon, 1993) may be crucial for the export process to occur. The relocation of proteins from the ER lumen to the cytoplasmic side of the ER membrane (in the opposite direction to the classically described pathway of protein import into the ER) remains to be investigated. Although the proposed mechanism is highly speculative, its appeal resides in the fact that a machinery provided by the host cell at the level of the ER membrane (A) can recognize a broad array of sequences similar to ShTA(220−246) and (B) can transport large proteins across this membrane barrier in association with ribosomes which (C) are the target site for the action of the catalytic A_1 domain.

The ShT A subunit lacks any ER retention sequences (RDEL/KDEL) found in other toxins and is presumably not responsible for the ER localization of the holotoxin. This is evident from experiments with FITC-labeled SLT-1 B subunit, where the internalized B subunit was found to be transported to the same compartments as the holotoxin (Khine & Lingwood, 1994). There is also the observation that acidic pH does not dissociate the B subunit from the receptor in a solid phase binding assay (Saleh & Gariépy, 1993). It is therefore apparent that localization of ShT is coupled to the movement of the receptor to the ER, the site of biosynthesis of ceramide [short review by Dawidowicz (1993)]. The B subunit may thus bring the A_1 fragment in close proximity to the ER membrane, as it remains bound to the receptor. In the context of membrane insertion of the A_1 fragment of ShT, our results show that it is possible for the C-terminus to play a role in the insertion/translocation of the A_1 fragment across the ER membrane.

ACKNOWLEDGMENT

We thank Godha Rangaraj for the operation of the Varian EPR spectrometer, Dr. Robert Hodges and Mr. Lorne Burke (Department of Biochemistry, University of Alberta) for performing mass spectrometry on the purified peptides, and Dr. Avi Chakrabartty for his help and access to his circular dichroism spectrometer and fluorometer.

REFERENCES

Bilge, A., Warner, C. V., & Press, O. W. (1995) *J. Biol. Chem. 270*, 23720−23725.

Blewitt, M. G., Chung, L. A., & London, E. (1985) *Biochemistry 24*, 5458−5464.

Blum, J. S., Fiani, M. L., & Stahl, P. D. (1991) *J. Biol. Chem. 266*, 22091−22095.

Bollen, I. C., & Higgins, J. A. (1980) *Biochem. J. 189*, 475−480.

Briggs, M. S., & Gierash, L. M. (1986) *Adv. Protein Chem. 38*, 109−180.

Burgess, B. J., & Roberts, L. M. (1993) *Mol. Microbiol. 10*, 171−179.

Choe, S., Bennett, M., Fujii, G., Curmi, P. M. G., Kantardjieff, K. A., Collier, R. J., & Eisenberg, D. (1992) *Nature 357*, 216−222.

Dawidowicz, E. A. (1993) *Curr. Opin. Struct. Biol. 3*, 495−498.

Donovan, J. J., Simon, M. I., Draper, R. K., & Montal, M. (1981) *Proc. Natl. Acad. Sci. U.S.A. 78*, 172−176.

Eletr, S., & Keith, A. D. (1972) *Proc. Natl. Acad. Sci. U.S.A. 69*, 1353−1357.

Endo, Y., Tsurugi, K., Yutsudo, T., Takeda, Y., Ogasawara, T., & Igarashi, K. (1988) *Eur. J. Biochem. 171*, 45−50.

Engelman, D. M., Steitz, T. A., & Goldman, A. (1986) *Annu. Rev. Biophys. Biophys. Chem. 15*, 321−353.
Falnes, P. O., Madshus, I. H., Sandvig, K., & Olsnes, S. (1992) *J. Biol. Chem. 267*, 12284−12290.
Farahbahksh, Z. T., & Wisnieski, B. J. (1989) *Biochemistry 28*, 580−585.
Fraser, M. E., Chernaia, M. M., Kozlov, Y. V., & James, M. N. G. (1994) *Nat. Struct. Biol. 1*, 59−64.
Garred, O., van Deurs, B., & Sandvig, K. (1995a) *J. Biol. Chem. 270*, 10817−10821.
Garred, O., Dubinina, E., Holm, P. K., Olsnes, S., van Deurs, B., Kozlov, J. V., & Sandvig, K. (1995b) *Exp. Cell Res. 218*, 39−49.
Gaut, J. R., & Hendershot, L. M. (1993) *Curr. Opin. Cell Biol. 5*, 589−595.
Gething, M. J., & Sambrook, J. (1992) *Nature 355*, 33−45.
Gordon, V. M., & Leppla, S. H. (1994) *Infect. Immun. 62*, 333−340.
Greenfield, N., & Fasman, G. D. (1969) *Biochemistry 8*, 4108−4116.
Hu, V. W., & Holmes, R. K. (1984) *J. Biol. Chem. 259*, 12226−12233.
Ishida, B., Cawley, D. B., Reue, K., & Wisnieski, B. (1983) *J. Biol. Chem. 258*, 5933−5937.
Jacewicz, M., Clausen, H., Nudelman, E., Donohue-Rolf, A., & Keusch, G. T. (1986) *J. Exp. Med. 163*, 1391−1404.
Khine, A. A., & Lingwood, C. A. (1994) *J. Cell. Physiol. 161*, 319−332.
Lakowicz, J. R. (1983) *Principles of Fluorescence Spectroscopy*, Plenum Press, New York.
Lindberg, A. A., Brown, J. E., Stromberg, N., Westling-Ryd, M., Schultz, J. E., & Karlsson, K. A. (1987) *J. Biol. Chem. 262*, 1770−1785.
Ludtke, S. J., He, K., Wu, Y., & Huang, H. W. (1994) *Biochim. Biophys. Acta 1190*, 181−184.
Markland, W., Cheng, S. H., Oostra, B. A., & Smith, A. E. (1986) *J. Virol. 59*, 82−89.
Mayer, L. D., Hope, M. J., Cullis, P. R., & Janoff, A. S. (1985) *Biochim. Biophys. Acta 817*, 193−196.
Merritt, E. A., & Hol, W. G. J. (1995) *Curr. Opin. Struct. Biol. 5*, 165−171.
Moskaug, J. O., Stenmark, H., & Olsnes, S. (1991) *J. Biol. Chem. 266*, 2652−2659.
O'Brien, A. D., & Holmes, R. K. (1987) *Microbiol. Rev. 51*, 206−220.
Perlman, D., & Halvorson, H. O. (1983) *J. Mol. Biol. 167*, 391−409.
Persson, B., & Argos, P. (1994) *J. Mol. Biol. 237*, 182−192.
Rolf, J. M., & Eidels, L. (1993) *Infect. Immun. 61*, 994−1003.
Rost, B., Casadio, R., Fariselli, P., & Sander, C. (1995) *Protein Sci. 4*, 521−533.
Rouser, G., Fleischer, S., & Yamamoto, A. (1975) *Lipids 5*, 494−496.
Saleh, M. T., & Gariépy, J. (1993) *Biochemistry 32*, 918−922.
Sandvig, K., Prydz, K., Ryd, M., & van Deurs, B. (1991) *J. Cell Biol. 113*, 553−562.
Sandvig, K., Garred, O., Prydz, K., Kozlov, J. V., Hansen, S. H., & van Deurs, B. (1992) *Nature 358*, 510−512.
Saxena, S. K., O'Brien, A. D., & Ackerman, E. J. (1989) *J. Biol. Chem. 264*, 596−601.
Simon, S. (1993) *Curr. Opin. Cell Biol. 5*, 581−588.
Simpson, J. C., Lord, J. M., & Roberts, L. M. (1995) *Eur. J. Biochem. 232*, 458−463.
Spiess, M., & Lodish, H. F. (1986) *Cell 44*, 177−185.
Takao, T., Tanabe, T., Hong, Y.-M., Shimonishi, Y., Kurazono, H., Yutsudo, T., Sasakawa, C., Utsumi, T., Ide, A., & Funatsu, G. (1989) *FEBS Lett. 242*, 255−258.
Utsumi, T., Aizono, Y., & Funatsu, G. (1984) *Biochim. Biophys. Acta 772*, 202−208.
Wang, Z., Jones, J. D., Rizo, J., & Gierasch, L. M. (1993) *Biochemistry 32*, 13991−13999.
Wetlaufer, D. B. (1962) *Adv. Protein Chem. 17*, 303−390.
Wharton, S. A., Martin, S. R., Ruigrok, R. W. H., Skehel, J. J., & Wiley, D. C. (1988) *J. Gen. Virol. 69*, 1847−1857.
Yamasaki, N., Nagase, Y., & Funatsu, G. (1988) *Agric. Biol. Chem. 52*, 1021−1026.
Zachowski, A. (1993) *Biochem. J. 294*, 1−14.
Zhan, H., Oh, K. J., Shin, Y.-K., Hubbel, W. L., & Collier, R. J. (1995) *Biochemistry 34*, 4856−4863.

BI960177Z